Cell Reports, Volume *17*

Supplemental Information

Robust Replication Control Is Generated by Temporal Gaps between Licensing and Firing Phases and Depends on Degradation of Firing Factor Sld2

Karl-Uwe Reusswig, Fabian Zimmermann, Lorenzo Galanti, and Boris Pfander

Figure S1. Related to Figure 1.

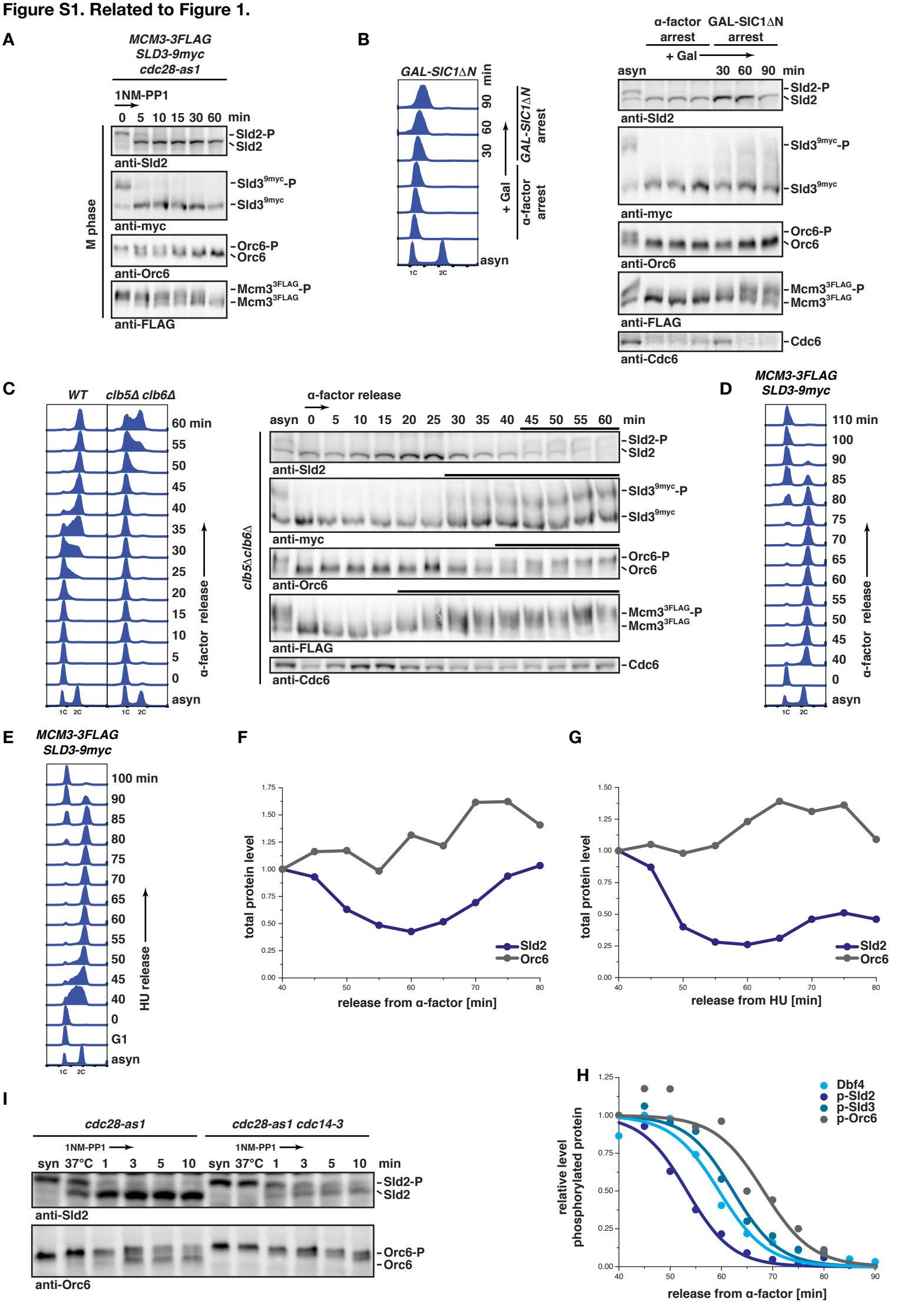

Figure S2. Related to Figure 2.

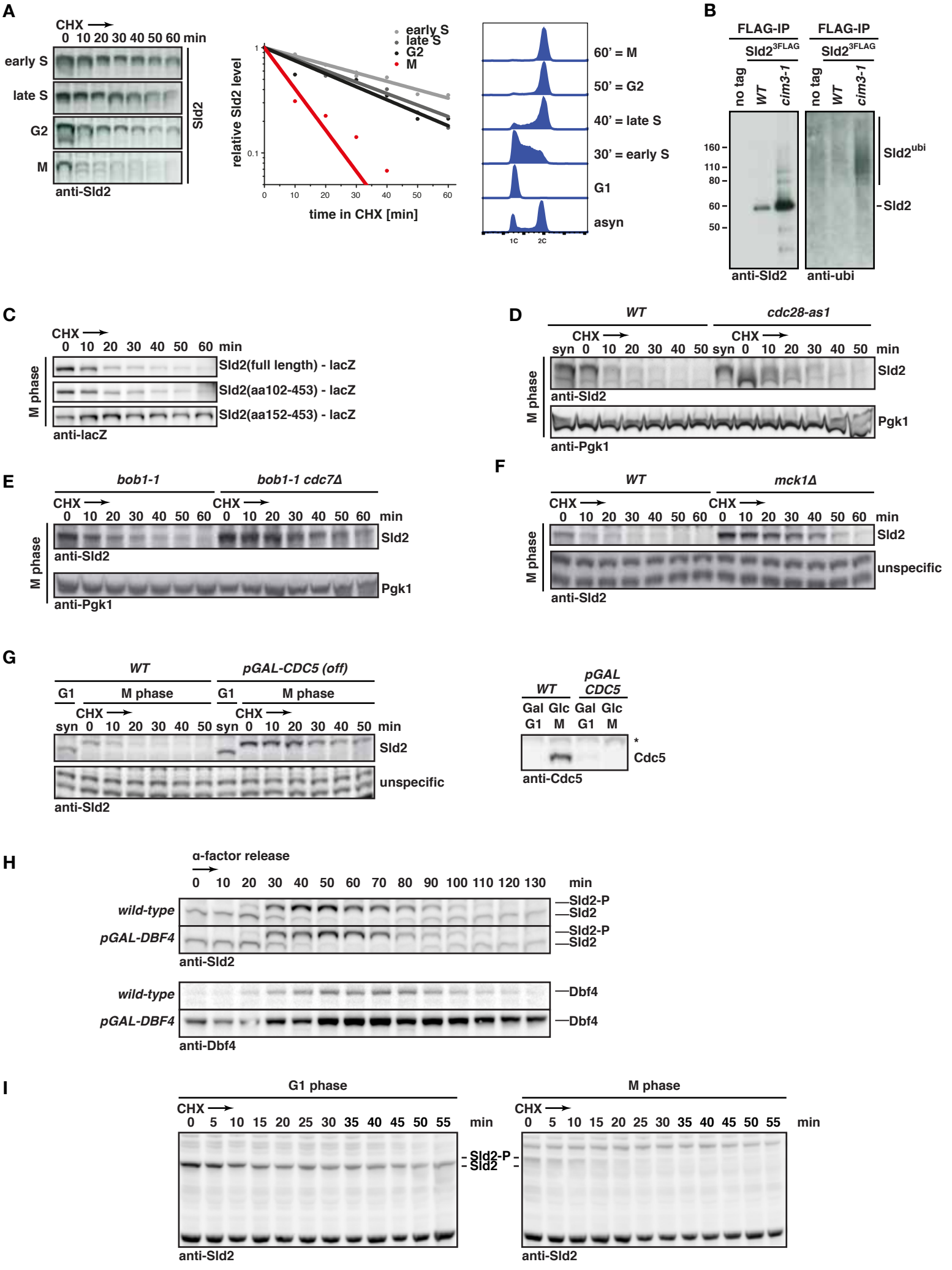

Figure S3. Related to Figure 3.

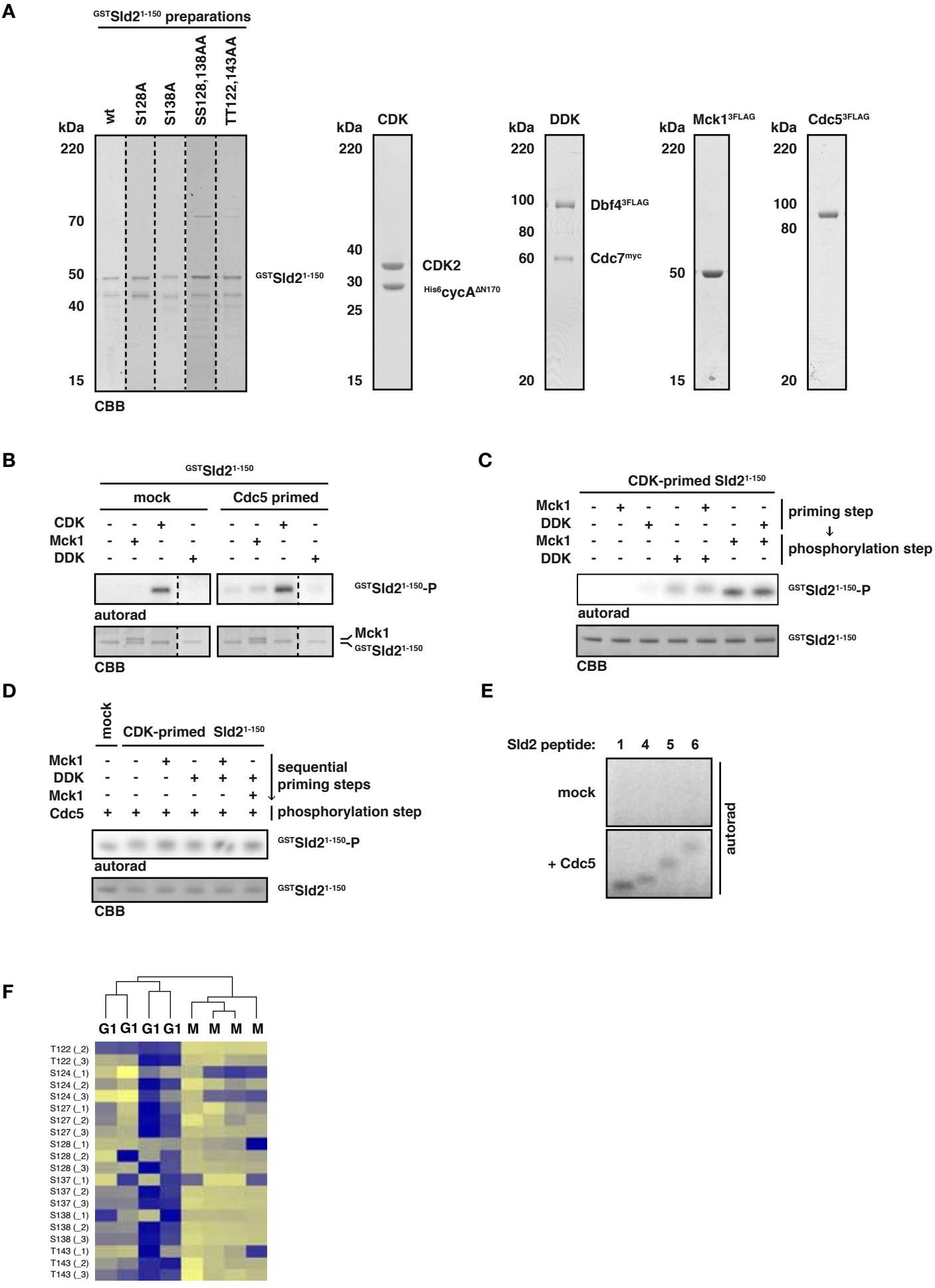

Figure S4. Related to Figure 4.

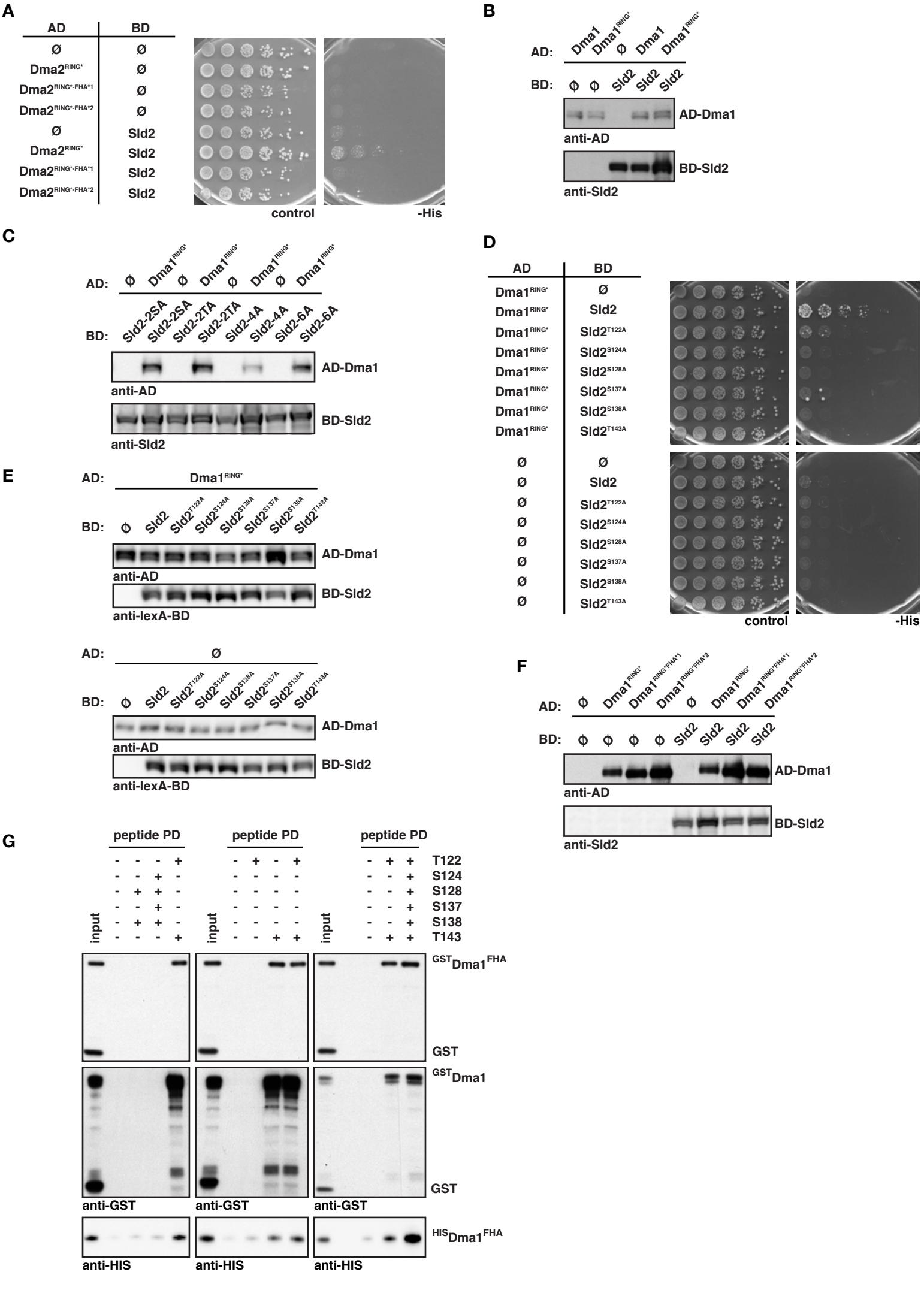

Figure S5. Related to Figure 5.

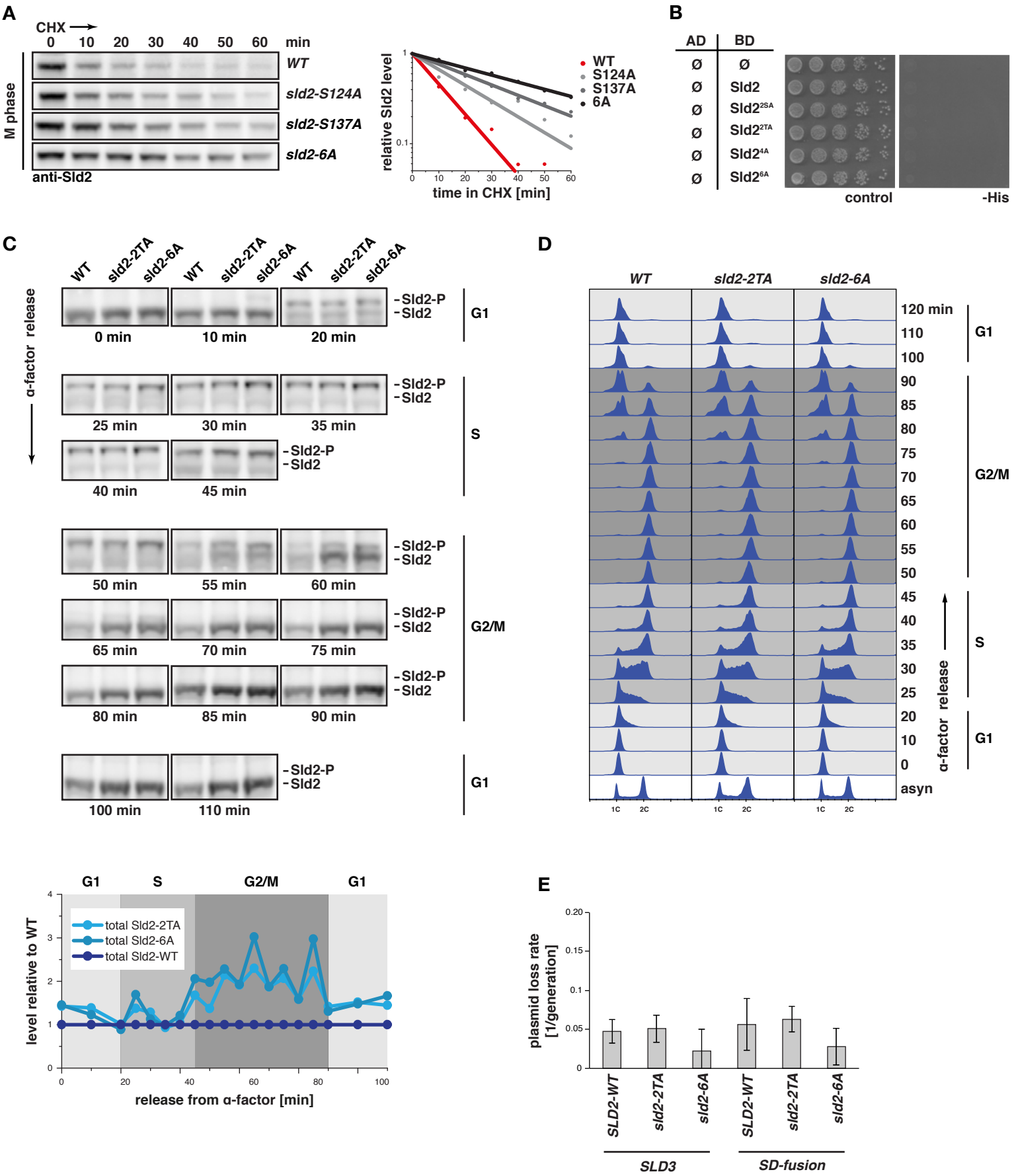

Figure S6. Related to Figure 6.

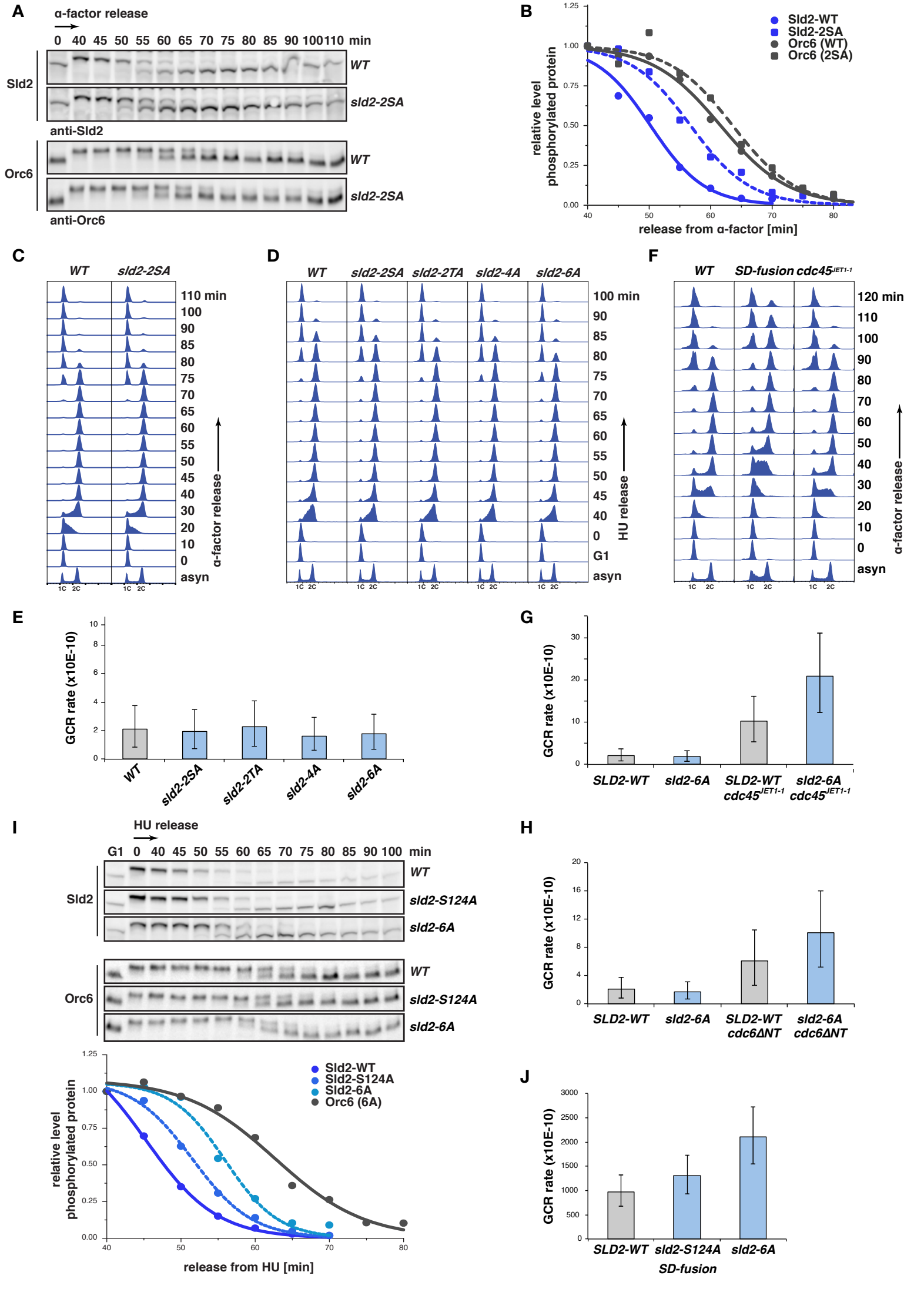

SUPPLEMENTAL FIGURE LEGENDS

Figure S1. Related to Figure 1.
Characterization of temporal gaps separating licensing and firing phases in G1 and M phase.

(A) Phosphorylation-dependent shifts in electrophoretic mobility of Sld2, Sld3, Orc6 and Mcm3 are dependent on CDK. *MCM3-3FLAG SLD3-9myc cdc28-as1* cells were arrested in M phase with nocodazole and treated with 1NM-PP1. Western blot- and Phostag-based visualization of hyper- and hypo-phosphorylated protein species was done as described in methods section.
(B) Cells arrested at the G1-S transition by *GAL-SIC1ΔN* overexpression show hyper-phosphorylated Mcm3 and low levels of Cdc6 indicating that these proteins are readily targeted by Cln-CDK, whereas Sld2, Sld3 and Orc6 are not hyper-phosphorylated and therefore exclusive Clb-CDK targets. DNA content measurement by flow cytometry (left panel) and measurement of protein phosphorylation and levels (right panel).
(C) Cln-CDK dependent phosphorylation of Mcm3 and degradation of Cdc6 occur before Clb-CDK dependent phosphorylation of Sld2, Sld3 and Orc6 in *clb5Δ clb6Δ* cells released from G1 arrest. DNA content measurement by flow cytometry (left panel) and measurement of protein phosphorylation and levels (right panel) as in **(A,B)**. Black bars above the blots indicate the presence of CDK hyper-phosphorylated protein species.
(D, E) Flow cytometric analyses of DNA content for α-factor (Fig. 1A-C) and HU (Fig. 1D-F) release experiments.
(F, G) Quantification of Sld2 and Orc6 total protein levels from α-factor (Fig. 1A-C) and HU (Fig. 1D-F) release experiments.
(H) Quantification of phosphorylated species of Sld2, Sld3, and Orc6 as well as total Dbf4 protein levels in cells released from G1 arrest (Fig. 1A-C)
(I) Sld2 is quickly reset to the hypo-phosphorylated form after CDK inhibition in *WT* and *cdc14-3* cells. *cdc28-as1* and *cdc28-as1 cdc14-3* cells were arrested in M phase, shifted to 37°C for 1h and treated with 1NM-PP1 for indicated times. Sld2 and Orc6 phosphorylation was measured as in **(A)**.

Figure S2. Related to Figure 2.
Requirements of Sld2 degradation.

(A) Measurement of Sld2 stability using cycloheximide (CHX) protein translation shut-offs and using cells released from G1 (α-factor) treated with cycloheximide 30 min (early S), 40 min (late S), 50 min (G2) and 60 min (M) post release. Measurement of Sld2 protein levels by western blot (left panel), quantification of Sld2 protein stability (middle panel) and flow cytometric analysis of DNA content (right panel).
(B) Ubiquitylated Sld2 species accumulate in the proteasome mutant *cim3-1*. Anti-FLAG immunoprecipitation from untagged control cells or *WT* or *cim3-1* cells harbouring $Sld2^{3FLAG}$ arrested in M phase and shifted to 37 °C for 2 h. Ubiquitylated Sld2 species of higher molecular weight are visualized by anti-Sld2 and anti-ubiquitin western blots. Note the increased Sld2 protein levels in the *cim3-1* mutant.
(C) Mapping of the Sld2 degron: the stability of truncated variants of the Sld2 protein from cells arrested in M phase is determined by protein translation shut-off. Stable versions of Sld2 include Sld2Δ152-453, but not Sld2Δ102-453 suggesting that the degron of Sld2 is positioned between aa102 and aa152.
(D-G) Full western blots of Sld2 CHX shut-off experiments in kinase mutant backgrounds shown in Fig. 2C-F, including Pgk1 loading control and an anti-Cdc5 western blot **(G)** that shows efficient Cdc5 expression shut-off after glucose (Glc) addition to the *pGALL-CDC5* strain.
(H) Overexpression of Dbf4 does not trigger premature Sld2 degradation. Cells were grown in YPGal and released from α-factor arrest. After all cells entered S phase, α-factor was added back to the culture. Sld2 and Dbf4 levels were monitored by western blot. Sld2 degradation is still restricted to mitosis in Dbf4-overexpressing cells, but it appears to occur slightly more efficiently as compared to wild-type cells.
(I) Larger images of the Sld2 western blots shown in Fig. 2A.

Figure S3. Related to Figure 3.
Phosphorylation of Sld2 by CDK, DDK, Mck1 and Cdc5 in vitro and in vivo.

(A) Recombinant purified proteins used in the in vitro phosphorylation assays: $^{GST}Sld2^{1-150}$ and mutant versions, CDK2-$^{His6}cycA^{\Delta N170}$ (CDK), $Cdc7^{myc}$-$Dbf4^{3FLAG}$ (DDK), $Mck1^{3FLAG}$ and $Cdc5^{3FLAG}$ were visualized by PAGE and CBB staining.
(B) Cdc5 priming has little influence on Sld2 phosphorylation by Mck1, CDK and DDK in vitro. In a priming step $^{GST}Sld2^{1-150}$ was phosphorylated with $Cdc5^{3FLAG}$ and non-radioactive ATP before treatment with the other kinases in a separate reaction in the presence of [γ^{32}P]-ATP as in Fig. 3A-B.

(C) Phosphorylation of Sld2 by Mck1 or DDK is not influenced by the other kinase. CDK-phosphorylated Sld2 is subjected to a second consecutive priming phosphorylation step using either Mck1 or DDK, before Mck1 and DDK phosphorylation is analysed in a third step in the presence of [γ^{32}P]-ATP.
(D) Cdc5-dependent phosphorylation of Sld2 is not influenced by any combination of priming phosphorylation using CDK, Mck1 or DDK. Starting with CDK priming, ^{GST}Sld2$^{1-150}$ was subjected to up to three consecutive priming phosphorylation steps, before Cdc5 phosphorylation of ^{GST}Sld2$^{1-150}$ was tested in the presence of [γ^{32}P]-ATP.
(E) Phosphorylation of synthetic Sld2 degron peptide at the CDK, Mck1 and DDK sites is not inhibitory to phosphorylation by Cdc5. An unphosphorylated control or phosphorylated Sld2 peptides (numbers as in Fig. 3D) were incubated with Cdc5 in the presence of [γ^{32}P]-ATP.
(F) The Sld2 degron is phosphorylated in vivo in a cell cycle-dependent manner. The heat map illustrates relative abundance of specific phosphorylated Sld2 peptides in a label free mass spectrometry experiment. Sld2 was enriched from cells arrested in G1 or M phase, with blue indicating low abundance and yellow indicating high abundance. Plotted are values that are normalized to total Sld2 levels in each sample from the four biological replicates. Each phosphorylation site is indicated by position. _1 refers to abundance of a given site in a singly phosphorylated state, _2 refers to peptides carrying two phosphorylated marks, _3 refers to peptides carrying three or more phosphorylated marks. The underlying Sld2 phosphorylation site table can be found as Table S2.

Figure S4. Related to Figure 4.
Additional two-hybrid interaction tests and expression controls to the Dma1/2-Sld2 interaction.

(A) Binding of Dma2 to Sld2 is dependent on the FHA domain of Dma2. Cells expressing lexA-BD empty and lexA-BD-Sld2 constructs as well as Gal4-AD empty, Gal4-AD-Dma2, Gal4-AD-Dma2-CH451,456SA (Dma2^{RING*}), Gal4-AD-Dma2- GCH298,451,456ESA (Dma2^{RING*FHA*1}) and Gal4-AD-Dma2-SHCH326,329,451,456ALSA (Dma2^{RING*FHA*2}) constructs were tested in two-hybrid assays.
(B,C,F) Expression control for two-hybrid assays from Fig. 4B-D. Two-hybrid constructs were detected with anti-AD (AD-Dma1 and mutant derivatives) or anti-Sld2 (BD-Sld2 and mutant derivatives) antibodies.
(D) All phosphorylation sites in the degron region are required for binding of Dma1 to Sld2. The two-hybrid analysis (Fig. 3C) was refined by using single point mutants of Sld2 phosphorylation sites.
(E) Expression control for two-hybrid assay in **(D)**. Two-hybrid constructs were detected with anti-AD (AD-Dma1^{RING*} and AD-empty) and anti-lexA-BD (BD-Sld2 and mutant derivatives) antibodies.
(G) Dma1 binds directly to phosphorylated versions of the Sld2 degron peptide. Biotinylated phospho-peptides of the Sld2 degron region were coupled to beads and used to pulldown Dma1 constructs either fused to GST or to a HIS-tag. The Dma1-fusion proteins were detected with anti-GST or anti-HIS antibodies.

Figure S5. Related to Figure 5.
Characterization of *sld2*-degron mutants.

(A) Cycloheximide (CHX) translation shut-off to determine Sld2 protein stability in M phase in *sld2*-degron mutant cells (*sld2-S124A* (lacking Mck1-phosphorylation site; *sld2-S137A* (lacking DDK-phosphorylation site), *sld2-6A = sld2-TSSSST122,124,128,137,138,143AAAAAA*). Left panel: anti-Sld2 western blots, right panel: quantification of Sld2 protein levels**.**
(B) Test of auto-activation of Sld2 constructs for the two-hybrid assay (used in Fig. 5D). Cells are expressing Gal4-AD empty, lexA-BD empty, lexA-BD-Sld2 and lexA-BD-Sld2 mutant constructs.
(C) Comparison of Sld2 protein levels in a *WT* strain or two strains each expressing stable versions of Sld2 (*sld2-2TA* = sld2-TT122,143AA; *sld2-6A* as in **(A)**). Cells were arrested in G1 with α-factor and released into fresh medium. Samples were taken at the indicated timepoints and α-factor was added back after 45 min of release. Quantification of total Sld2 protein levels relative to the *WT* Sld2 at the same timepoints is shown in the lower panel. Cell cycle phases are indicated by grey shading.
(D) Flow cytometric analysis of DNA content for the experiment shown in **(C)**. Cell cycle phases are indicated by grey shading.
(E) Plasmid loss rates of an ARS/CEN plasmid (pRS313) of *WT* and *sld2*-degron mutant strains in the background of either *SLD3 WT* or *SLD3-DPB11ΔN-fusion* (as in Fig. 5C). Values are average from two independent experiments; error bars indicate standard deviations.

Figure S6. Related to Figure 6.

Stabilized versions of Sld2 narrow the gap between firing and licensing phases in mitosis.

(A) Measurement of the gap between disappearance of CDK-phosphorylated Sld2 and CDK- phosphorylated Orc6 in *SLD2-WT* and *sld2-2SA* degron mutant cells released from G1 phase arrest.
(B) Quantification of the CDK-phosphorylated protein species from western blots in **(A)**.
(C-D) Flow cytometric analysis of DNA content to verify synchronous cell cycle progression after arrest/release **(C)** from α-factor (blots in **(A-B)**) or **(D)** from HU (blots in Fig. 6A-B).
(E) Stable Sld2 does not cause increased incidence of gross chromosomal rearrangements (GCR). Rates of GCR events were measured using the *CAN1::URA3* reporter on chromosome V in *WT* (grey) and *sld2*-degron mutant (blue) strains. GCR rates were calculated from eight fluctuations; error bars indicate a 95% confidence interval.
(F) *SLD3-DPB11ΔN-fusion* (*SD-fusion*) cells are partially defective in replication initiation. Flow cytometric analysis of the DNA content of *WT*, *SD-fusion* and *cdc45*$^{JET1\text{-}1}$ cells after arrest/release from α-factor.
(G,H) Stable Sld2 (blue) causes an increased incidence of GCR events in combination with mutations in other replication factors (*cdc45*$^{JET1\text{-}1}$ **(G)** or *cdc6ΔNT* **(J)**). GCR assays were performed as in **(E)**. GCR rates were calculated from eight fluctuations; error bars indicate a 95% confidence interval.
(I) The partially stabilized *sld2-S124A* mutant narrows the gap between firing inactivation and licensing activation to a lesser extent than the stable *sld2-6A* mutant. The experiment was performed as in Fig. 6A. Lower panel: Quantification of phosphorylated Sld2 species and phosphorylated Orc6.
(J) The partially stabilized *sld2-S124A* mutant increases the GCR rate to a lesser extent than the stable *sld2-6A* mutant in an *SD-fusion* background. GCR assays were performed as in Fig. 6D. GCR rates were calculated from eight fluctuations; error bars indicate a 95% confidence interval.

SUPPLEMENTAL TABLES

Table S1. Related to Figure 3 and Figure S3.
Phosphorylation sites of Sld2 in vivo.

Phosphorylation site table obtained with MaxQuant after MS analysis of Sld2 purified from mitotic cells. Sample 1 is from Sld2 expressed at endogenous levels; sample 2 is from Sld2 expressed from a strong promoter.

Table S2. Related to Figure 3 and Figure S3.
Phosphorylation sites of Sld2 in vivo in different cell cycle phases.

Phosphorylation site table obtained with MaxQuant after MS analysis of Sld2 purified from G1 phase cells and mitotic cells. Sld2 was expressed from a strong promoter. Samples 1-4 are biological replicates of Sld2 from G1 phase cells; samples 5-8 are biological replicates of Sld2 from mitotic cells.

SUPPLEMENTAL SPECTRA

Spectra S1. Related to Table S1 and Table S2.
MS-MS spectra of Sld2 phosphorylation sites in the Sld2 degron.

SUPPLEMENTAL EXPERIMENTAL PROCEDURES

Yeast strains

Yeast strains are based on W303 MATa and were constructed using standard methods (Janke et al., 2004). Cells were grown at 30°C except for the temperature-sensitive *cim3-1* and *cdc14-3* strains. Strains harbouring the *cim3-1* allele were grown and synchronized at 25°C and shifted to 37°C for 2 h to inactivate Cim3. Strains harbouring the *cdc14-3* allele were grown and synchronized at 25°C and shifted to 37°C for 1 h to inactivate Cdc14. Inhibition of the inhibitor-sensitive CDK allele *cdc28-as1* (Bishop et al., 2000) was performed by adding 1NM-PP1 (final concentration 1.5 µM, Merck) directly to the previously synchronized culture.

Strain	Relevant genotype	Source
W303a	MATa ade2-1 ura3-1 his3-11,15 trp1-1 leu2-3,112 can1-100	(Rothstein, 1983)
YKR554	W303a SLD3-9myc::HIS3MX6 MCM3-3FLAG::hph-NT1	this study
YKR633	W303a SLD3-9myc::HIS3MX6 MCM3-3FLAG::hph-NT1 cdc28-as1	this study
YKR575	W303a SLD3-9myc::HIS3MX6 MCM3-3FLAG::hph-NT1 ura3::pGAL-SIC1ΔNT::URA3	this study
YKR617	W303a SLD3-9myc::HIS3MX6 MCM3-3FLAG::hph-NT1 ura3::pGAL-SIC1ΔNT::URA3 clb5Δ::kanMX4 clb6Δ::nat-NT2	this study
YKR494	W303a cdc14-3 cdc28-as1	this study
YKR503	W303a sld2Δ::hph-NT1 SLD2(LEU2)	this study
YKR514	W303a sld2Δ::hph-NT1 $sld2^{\Delta 100-150}$(LEU2)	this study
YKR516	W303a sld2Δ::hph-NT1 $sld2^{\Delta 120-150}$(LEU2)	this study
YKR112	W303a cdc28-as1	this study
JD2042	W303a bob1-1::HIS3	John Diffley lab
YKR102	W303a bob1-1::HIS3 cdc7Δ::nat-NT2	this study
YKR090	W303a mck1Δ::hph-NT1	this study
YKR162	W303A pGALL-CDC5::kanMX4	this study
YKR060	W303a Sld2-3FLAG::hph-NT1	this study
YKR081	W303a cim3-1 Sld2-3FLAG::hph-NT1	this study
YTM02	W303a leu2::pSLD2-SLD2-lacZ::LEU2	this study
YKR166	W303a leu2::pSLD2-$SLD2^{102-453}$-lacZ::LEU2	this study
YKR714	W303a leu2::pSLD2-$SLD2^{152-453}$-lacZ::LEU2	this study
YFZ019	W303a pep4Δ::LEU2 his3::MCK1-3FLAG-pGAL1-10-GAL4::HIS3	this study
YFZ020	W303a pep4Δ::LEU2 his3::CDC5-3FLAG-pGAL1-10-GAL4::HIS3	this study
YFZ021	W303a pep4Δ::hph-NT1 LEU2::GAL-DBF4-3FLAG::KanMx CDC7-myc::TRP1 HIS3::pGal-GAL4	this study

YKR624	W303a dma1Δ::TRP1	this study
YKR625	W303a dma2Δ::TRP1	this study
YKR626	W303a dma1Δ::TRP1 dma2Δ::HIS3MX6	this study
L40	MATa his3Δ200 trp1-901 leu2-3,112 ade2 LYS2::(4 $lexA_{op}$-HIS3) URA3::(8 $lexA_{op}$-lacZ) GAL4	Invitrogen
YKR640	(L40 background) dma1Δ::nat-NT2 dma2Δ::hph-NT1	this study
YKR685	W303a CAN1::URA3 sld2Δ::hph-NT1 leu2::SLD2::LEU2	this study
YKR686	W303a CAN1::URA3 sld2Δ::hph-NT1 leu2::sld2-2SA::LEU2	this study
YKR687	W303a CAN1::URA3 sld2Δ::hph-NT1 leu2::sld2-2TA::LEU2	this study
YKR688	W303a CAN1::URA3 sld2Δ::hph-NT1 leu2::sld2-4A::LEU2	this study
YKR689	W303a CAN1::URA3 sld2Δ::hph-NT1 leu2::sld2-6A::LEU2	this study
YKR690	W303a CAN1::URA3 SLD3-DPB11ΔN-fusion::kanMX4 sld2Δ::hph-NT1 leu2::SLD2::LEU2	this study
YKR691	W303a CAN1::URA3 SLD3-DPB11ΔN-fusion::kanMX4 sld2Δ::hph-NT1 leu2::sld2-2SA::LEU2	this study
YKR692	W303a CAN1::URA3 SLD3-DPB11ΔN-fusion::kanMX4 sld2Δ::hph-NT1 leu2::sld2-2TA::LEU2	this study
YKR693	W303a CAN1::URA3 SLD3-DPB11ΔN-fusion::kanMX4 sld2Δ::hph-NT1 leu2::sld2-4A::LEU2	this study
YKR694	W303a CAN1::URA3 SLD3-DPB11ΔN-fusion::kanMX4 sld2Δ::hph-NT1 leu2::sld2-6A::LEU2	this study
YKR742	W303a CAN1::URA3::ARS306::nat-NT2 sld2Δ::hph-NT1 leu2::SLD2::LEU2 ars306Δ::HIS3MX6	this study
YKR743	W303a CAN1::URA3::ARS306::nat-NT2 SLD3-DPB11ΔN-fusion::kanMX4 sld2Δ::hph-NT1 leu2::SLD2::LEU2 ars306Δ::HIS3MX6	this study
YKR744	W303a CAN1::URA3::ARS306::nat-NT2 SLD3-DPB11ΔN-fusion::kanMX4 sld2Δ::hph-NT1 leu2::sld2-2SA::LEU2 ars306Δ::HIS3MX6	this study
YKR746	W303a CAN1::URA3::ARS306::nat-NT2 SLD3-DPB11ΔN-fusion::kanMX4 sld2Δ::hph-NT1 leu2::sld2-4A::LEU2 ars306Δ::HIS3MX6	this study
YKR747	W303a CAN1::URA3::ARS306::nat-NT2 SLD3-DPB11ΔN-fusion::kanMX4 sld2Δ::hph-NT1 leu2::sld2-6A::LEU2 ars306Δ::HIS3MX6	this study
YKR396	W303a sld2Δ::hph-NT1 leu2::sld2-2SA::LEU2	this study
YKR603	W303a sld2Δ::hph-NT1 leu2::sld2-2TA::LEU2	this study
YKR607	W303a sld2Δ::hph-NT1 leu2::sld2-4A::LEU2	this study
YKR612	W303a sld2Δ::hph-NT1 leu2::sld2-6A::LEU2	this study

YKR787	W303a ura3::pGAL-CDC5::URA3	this study
YKR897	W303a CAN1::URA3 sml1Δ::HIS3MX6 mec1Δ::nat-NT2	this study
YKR847	W303a CAN1::URA3 sml1Δ::HIS3MX6 mec1Δ::nat-NT2 sld2Δ::hph-NT1 leu2::sld2-6A::LEU2	this study
YKR872	W303a CAN1::URA3 sld2Δ::hph-NT1 leu2::SLD2::LEU2 trp1::pGAL-DBF4::TRP1	this study
YKR873	W303a CAN1::URA3 sld2Δ::hph-NT1 leu2::sld2-6A::LEU2 trp1::pGAL-DBF4::TRP1	this study
YKR882	W303a CAN1::URA3 sld2Δ::hph-NT1 leu2::SLD2::LEU2 bob1-1::HIS3	this study
YKR883	W303a CAN1::URA3 sld2Δ::hph-NT1 leu2::sld2-6A::LEU2 bob1-1::HIS3	this study
YKR781	W303a bar1Δ::TRP1 pep4Δ::LEU2 pGPD-SLD2-3FLAG::URA3,hph-NT1 lys1Δ::kanMX4 dma1Δ::HIS3MX6 dma2Δ::natNT2	this study
YKR813	W303a CAN1::URA3 sld2Δ::hph-NT1 leu2::sld2-S124A::LEU2	this study
YKR824	W303a CAN1::URA3 SLD3-DPB11ΔN-fusion::kanMX4 sld2Δ::hph-NT1 leu2::sld2-S124A::LEU2	this study
YKR814	W303a CAN1::URA3 sld2Δ::hph-NT1 leu2::sld2-S137A::LEU2	this study
YKR862	W303a CAN1::URA3 sld2Δ::hph-NT1 leu2::SLD2::LEU2 cdc45::JET1-1::TRP1	this study
YKR863	W303a CAN1::URA3 sld2Δ::hph-NT1 leu2::sld2-6A::LEU2 cdc45::JET1-1::TRP1	this study
YKR809	W303a CAN1::URA3 sld2Δ::hph-NT1 leu2::SLD2::LEU2 cdc6ΔNT::nat-NT2	this study
YKR810	W303a CAN1::URA3 sld2Δ::hph-NT1 leu2::sld2-6A::LEU2 cdc6ΔNT::nat-NT2	this study

Plasmids

Yeast genes of interest were amplified from genomic DNA of W303 and cloned into the respective vector using the In-Fusion HD cloning kit (Clontech). Mutations were introduced by oligonucleotide-directed site-directed mutagenesis.

plasmid number	description
pKR032	YCplac111 pSLD2-SLD2
pKR169	YCplac111 pSLD2-SLD2$^{\Delta 100\text{-}150}$
pKR170	YCplac111 pSLD2-SLD2$^{\Delta 120\text{-}150}$
pKR001	pRS406 cdc28-as1 (F88G), lacks ATG
pFZ025	pGEX-4T-1 SLD2$^{1\text{-}150}$
pFZ046	pGEX-4T-1 SLD2$^{1\text{-}150}$ S128A
pFZ047	pGEX-4T-1 SLD2$^{1\text{-}150}$ S138A
pFZ048	pGEX-4T-1 SLD2$^{1\text{-}150}$ S128A S138A (“2SA”)
pFZ051	pGEX-4T-1 SLD2$^{1\text{-}150}$ T122A T143A (“2TA”)
pFZ029	pRS303 MCK1-3FLAG pGAL1-10 GAL4
pFZ030	pRS303 CDC5-3FLAG pGAL1-10 GAL4
pKR245	pGEX-4T-1 DMA1
pKR314	pGEX-4T-1 DMA1$^{FHA\ (1\text{-}298)}$

pKR202	pACT2 DPB11 (GAL4-AD-DPB11)
pKR261	pACT2 DMA1 (GAL4-AD-DPB11)
pKR265	pACT2 DMA1^{RING*} (C345S H350A)
pKR290	pACT2 DMA1$^{RING* +FHA1*}$ (S220A H223L C345S H350A)
pKR291	pACT2 DMA1$^{RING* +FHA2*}$ (G192E C345S H350A)
pKR266	pACT2 DMA2^{RING*} (C451S H456A)
pKR292	pACT2 DMA2$^{RING*+FHA1*}$ (CS326A H329L C451S H456A)
pKR293	pACT2 DMA2$^{RING*+FHA1*}$ (G298E C451S H456A)
pKR204	pBTM116 SLD2 (lexA-BD-SLD2)
pKR276	pBTM116 sld2-2SA (S128A S138A)
pKR277	pBTM116 sld2-2TA (T122A T143A)
pKR278	pBTM116 sld2-4A (T122A S128A S138A T143A)
pKR279	pBTM116 sld2-6A (T122A S124A S128A S137A S138A T143A)
pKR016	YIplac128 pSLD2-SLD2
pKR064	YIplac128 pSLD2-sld2-2SA (S128A S138A)
pKR226	YIplac128 pSLD2-sld2-2TA (T122A T143A)
pKR228	YIplac128 pSLD2-sld2-4A (T122A S128A S138A T143A)
pKR231	YIplac128 pSLD2-sld2-6A (T122A S124A S128A S137A S138A T143A)
pKR087	YIplac211 CAN1
pKR244	pFA6a nat-NT2 ARS306
pLG01	pET28a DMA1$^{FHA(1-298)}$
pKR301	pBTM116 sld2-S124A
pKR302	pBTM116 sld2-S128A
pKR303	pBTM116 sld2-S138A
pKR304	pBTM116 sld2-T122A
pKR306	pBTM116 sld2-S137A
pKR307	pBTM116 sld2-T143A

Cell cycle arrest and release experiments

Cells were grown to log-phase (OD_{600} 0.5) in YP medium + 2% glucose (YPD) at 30°C (if not stated otherwise) prior to arrest. To arrest cells in G1, the culture was supplemented with α-factor (final concentration 5 µg/ml, synthesized at MPIB core facility) for 1:45 h. To arrest cells in G2/M, the culture was supplemented with nocodazole (final concentration 5 µg/ml, Sigma-Aldrich) for 2 h. To arrest cells in early S phase, the culture was first arrested in G1 as described above and then released to fresh YPD supplemented with 200 mM hydroxyurea (HU) for 1 h.

Release from G1 or HU arrests were performed by washing the cells with pre-warmed YPD once followed by re-suspending the cells in pre-warmed YPD. To ensure that cells run through the cell cycle only once, alpha-factor (final concentration 5 µg/ml) was added back to the medium 40 min after the release (G1 releases) or directly after re-suspending the cells in fresh YPD (HU releases).

For subsequent analysis, samples (1 OD, approx. $2x10^7$ cells) were withdrawn from the cultures according to the time course of the experiment. For flow cytometric analysis, the cells were re-suspended in FACS buffer (70% ethanol, 50 mM Tris pH 8.0) and kept at 4°C at least for 1 h prior to further processing (see subsection "Flow cytometry"). For western blot analysis, the cells were snap-frozen in liquid nitrogen and stored at -80°C prior to further processing (see subsection "Preparation of whole cell extracts (alkaline lysis/TCA)").

Protein translation shutoff experiments using cycloheximide (CHX)

Cells were grown to log-phase (OD_{600} 0.5) and arrested with either alpha-factor or nocodazole. Then, cycloheximide (CHX, Sigma, final concentration 500 µg/ml) was added to the culture to block further protein translation and monitor ongoing degradation processes. For western blot analysis, samples (1 OD, approx. $2x10^7$ cells) were withdrawn from the cultures according to the time course of the experiment and snap-frozen in liquid nitrogen. In addition, samples for flow cytometric analysis were withdrawn from the cultures before the addition of every drug and at the end of the experiment.

Preparation of whole cell extracts (alkaline lysis/TCA)

Cell pellets were re-suspended in 1 ml pre-cooled H_2O and incubated with 150 µl of freshly prepared lysis solution (1.85 M NaOH, 7.5% beta-mercaptoethanol) at 4°C for 15 min. Then, the lysate was admixed with 150 µl 55% trichloroacetic acid (TCA) and incubated at 4°C for 10 min. After centrifugation and careful aspiration of the supernatant, the precipitated proteins were re-suspended in 50 µl HU-buffer (8 M urea, 5% SDS, 200 mM Tris pH 6.8, 1.5% dithiothreitol, traces of bromophenol blue) and incubated at 65°C for 10 min.

Yeast two-hybrid analysis

The plasmids used for yeast two-hybrid analysis in this study were based on pACT2 (Clontech) and pBTM116 (Clontech). To assay for an interaction between Sld2 and Dpb11, respective plasmids were transformed into L40 cells (Invitrogen) as described previously (Tak et al., 2006). To assay for an interaction between Sld2 and Dma1/Dma2, respective plasmids were transformed into YKR640 cells (*dma1*Δ *dma2*Δ in the L40 background). Transformants were spotted in serial dilution (1:5) either on SC-Leu-Trp plates (control) or on SC-Leu-Trp-His plates (selection) and incubated at 30°C for 2-4 days. Cells from the control plates were then grown in SC-Leu-Trp to log-phase to take samples for subsequent analysis of the expression of the AD-/BD-fusion proteins by western blot.

Plasmid loss assay

Cells were transformed with YCplac33 and grown to saturation (i.e. 10^8 cells/ml in SC-Ura medium. Fresh YPD medium was inoculated with 10^5 cells and grown overnight to saturation (approximately 11 generations). After dilution (1:10,000), 100 µl were plated on YPD and SC-Ura plates and colonies were counted after incubation for 2 days at 30°C. Two or three independent experiments were performed to calculate the mean plasmid loss rate per generation.

Gross chromosomal rearrangement (GCR) assay

Strains were transformed with a reporter cassette containing *CAN1::URA3* that was integrated into the *can1* locus on chromosome V to allow for a measurement of GCR rates. The GCR assay was performed as described (Putnam and Kolodner, 2010). Briefly, cells were grown in SC-Ura overnight and then plated out for single colonies on YPD. These single colonies were used to inoculate larger cultures. Strains harboring the *SLD3-DPB11*Δ*N-fusion* allele were grown in 2 ml YPD to saturation; all other strains were grown in 50 ml YPD to saturation. A dilution of the culture (100 µl of 1:100,000) was plated on YPD in duplicates and the remainder was plated on SC-Arg plates containing 5'-fluoroorotic acid (5-FOA, final concentration 1000 mg/L, US Biological Life Sciences) and L-canavanine (Cana, final concentration 50 mg/L, Sigma-Aldrich) and incubated at 30°C. Colonies on YPD plates were counted after 2 days; colonies on SC-Arg+Cana+5-FOA were counted after 5 days.

Fluctuation analysis of the acquired data was performed using FALCOR (Hall et al., 2009). The calculations were performed with the Ma-Sandri-Sarkar Maximum Likelihood Estimator (MSS-MLE) method. Confidence intervals (95%) for the calculated GCR rates were determined as described in the literature (Rosche and Foster, 2000; Stewart, 1994). The use of the MSS-MLE allows comparing GCR event estimators in two-tailed Student's t-tests (Stewart, 1994). These calculations were performed with the web-tool "GraphPad QuickCalc t test calculator" (http://www.graphpad.com/quickcalcs/ttest2). The tables below summarize the calculated p-values for individual panels in Figure 6 and Supplemental Figure 6.

Figure 6C

	MEC1 SML1 SLD2-WT	***MEC1 SML1 sld2-6A***	***mec1*Δ *sml1*Δ *SLD2-WT***	***mec1*Δ *sml1*Δ *sld2-6A***
MEC1 SML1 SLD2-WT	/	1	< 0.0001	< 0.0001
MEC1 SML1 sld2-6A	1	/	< 0.0001	< 0.0001
mec1*Δ *sml1*Δ *SLD2-WT	< 0.0001	< 0.0001	/	< 0.0001
mec1*Δ *sml1*Δ *sld2-6A	< 0.0001	< 0.0001	< 0.0001	/

Figure 6D

		SLD3	***SD-fusion***				
	SLD2	***WT***	***WT***	***2SA***	***2TA***	***4A***	***6A***
SLD3	***WT***	/	< 0.0001	< 0,0001	< 0.0001	< 0.0001	< 0.0001
SD-fusion	***WT***	< 0.0001	/	< 0.0001	< 0.0001	< 0.0001	< 0.0001
	2SA	< 0.0001	< 0.0001	/	0.8742	0.3375	0.6711
	2TA	< 0.0001	< 0.0001	0.8742	/	0.2676	0.5614
	4A	< 0.0001	< 0.0001	0.3375	0.2676	/	0.5846
	6A	< 0.0001	< 0.0001	0.6711	0.5614	0.5846	/

Figure 6E

		pGAL-DBF4 (glucose)		***pGAL-DBF4 (galactose)***	
		SLD2-WT	***sld2-6A***	***SLD2-WT***	***sld2-6A***
pGAL-DBF4 (glucose)	***SLD2-WT***	/	0.6423	< 0.0001	< 0.0001
	sld2-6A	0.6423	/	0.0002	< 0.0001
pGAL-DBF4 (galactose)	***SLD2-WT***	< 0.0001	0.0002	/	< 0.0001
	sld2-6A	< 0.0001	< 0.0001	< 0.0001	/

Figure 6F (part 1)

		CAN1::URA3 SD-fusion			
		SLD2-WT	***sld2-2SA***	***sld2-4A***	***sld2-6A***
CAN1::URA3 SD-fusion	***SLD2-WT***	/	< 0.0001	< 0.0001	< 0.0001
	sld2-2SA	< 0.0001	/	0.4734	0.0002
	sld2-4A	< 0.0001	0.4734	/	0.001
	sld2-6A	<0,0001	0,0002	0,001	/
CAN1::URA3::ARS306 SD-fusion	***SLD2-WT***	0.0004	< 0.0001	< 0.0001	< 0.0001
	sld2-2SA	< 0.0001	0.0002	< 0.0001	< 0.0001
	sld2-4A	< 0.0001	< 0.0001	< 0.0001	< 0.0001
	sld2-6A	< 0.0001	0.0004	< 0.0001	< 0.0001

Figure 6F (part 2)

		CAN1::URA3::ARS306 SD-fusion			
		SLD2-WT	***sld2-2SA***	***sld2-4A***	***sld2-6A***
CAN1::URA3 SD-fusion	***SLD2-WT***	0.0004	< 0.0001	< 0.0001	< 0.0001
	sld2-2SA	< 0.0001	0.0002	< 0.0001	0.0004
	sld2-4A	< 0.0001	< 0.0001	< 0.0001	< 0.0001
	sld2-6A	< 0.0001	< 0.0001	< 0.0001	< 0.0001
CAN1::URA3::ARS306 SD-fusion	***SLD2-WT***	/	< 0.0001	< 0.0001	< 0.0001
	sld2-2SA	< 0.0001	/	0.4291	0.7553
	sld2-4A	< 0.0001	0.4291	/	0.2766
	sld2-6A	< 0.0001	0.7553	0.2766	/

Figure S6E

	SLD2-WT	***sld2-2SA***	***sld2-2TA***	***sld2-4A***	***sld2-6A***
SLD2-WT	/	0.6528	0.7802	0.7749	1
sld2-2SA	0.6528	/	0.8634	0.8689	0.6528
sld2-2TA	0.7802	0.8634	/	0.9945	0.7802
sld2-4A	0.7749	0.8689	0.9945	/	0.7749
sld2-6A	1	0.6528	0.7802	0.7749	/

Figure S6G

	CDC45 SLD2-WT	***CDC45 sld2-6A***	***cdc45^{JET1-1} SLD2-WT***	***cdc45^{JET1-1} sld2-6A***
CDC45 SLD2-WT	/	1	0.0001	< 0.0001
CDC45 sld2-6A	1	/	0.0001	< 0.0001
cdc45^{JET1-1} SLD2-WT	0.0001	0.0001	/	< 0.0001
cdc45^{JET1-1} sld2-6A	< 0.0001	< 0.0001	< 0.0001	/

Figure S6H

	CDC6 SLD2-WT	***CDC6 sld2-6A***	***cdc6ΔNT SLD2-WT***	***cdc6ΔNT sld2-6A***
CDC6 SLD2-WT	/	1	0.0157	< 0.0001
CDC6 sld2-6A	1	/	0.0157	< 0.0001
cdc6ΔNT SLD2-WT	0.0157	0.0157	/	0.0006
cdc6ΔNT sld2-6A	< 0.0001	< 0.0001	0.0006	/

Figure S6J

	SD-fusion SLD2-WT	***SD-fusion sld2-S124A***	***SD-fusion sld2-6A***
SD-fusion SLD2-WT	/	0.0042	< 0.0001
SD-fusion sld2-S124A	0.0042	/	< 0.0001
SD-fusion sld2-6A	< 0.0001	< 0.0001	/

Flow cytometry

Fixed samples for flow cytometry (in FACS buffer) were washed once with 50 mM Tris pH 8.0, re-suspended in 520 µl RNAse solution (500 µl 50 mM Tris pH 8.0 supplemented with 20 µl RNAseA (10 mg/ml in 10 mM Tris pH 7.5, 10 mM $MgCl_2$)) and incubated at 37°C overnight. Next, the samples were washed once with 50 mM Tris pH 8.0, re-suspended in 220 µl proteinase K solution (200 µl 50 mM Tris pH 8.0 supplemented with 20 µl proteinase K (10 mg/ml in 50% glycerol, 10 mM Tris pH 7.5, 25 mM $MgCl_2$)) and incubated at 50°C for 30 min. After this digestion, the samples were re-suspended in 500 µl 50 mM Tris pH 8.0 and sonified. The sonified samples were diluted 1:20 in SYTOX buffer (50 mM Tris pH 8.0, 1 µM SYTOX green) and 10,000 cells per sample were analysed on a MACSquant Analyzer 10 flow cytometer (Miltenyi Biotec). The SYTOX green signal was measured in the B1 channel (linear mode). Flow cytometry data was analysed with the software FlowJo v10.0.8 (FlowJo, LLC).

Protein purification

CDK, $^{GST}Sld2^{1-150}$ variants, $^{GST}Dma1$, $^{GST}Dma1^{FHA}$ and $^{HIS}Dma1^{FHA}$ were expressed in *E. coli* BL21 pRIL cells (Agilent). Mck1, DDK and Cdc5 were overexpressed in *S. cerevisiae* from a galactose-inducible GAL1-10 promoter. All purification steps were performed on ice or at 4°C.

Purification of bacterially expressed CDK2/cycA$^{\Delta N170}$

To generate CDK2/cycA$^{\Delta N170}$ complex, $^{GST}CDK2$ and $^{His6}cycA^{\Delta N170}$ were expressed separately. Bacteria with either expression plasmids were grown in 1 L LB medium supplemented with antibiotics to mid-log phase. Both cultures were cooled down on ice for 5 min to increase chaperone expression followed by addition of 1 mM IPTG and incubation for 20 h at 20°C. Cells were pelleted and resuspended in 40 mL Lysis Buffer B2 (300 mM NaCl, 20 mM HEPES pH 7.6, 5 mM β-mercaptoethanol, 0.01% NP-40, 100 µM AEBSF, 1x complete protease inhibitor cocktail EDTA-free) followed by lysis with an EmulsiFlex-C3 system for three rounds at 1,000 bar. Cell debris was spun down at 140,000 g for 45 min. To allow complex formation between both subunits, extracts were pooled and incubated for 45 min. For glutathione affinity chromatography, 1 mL bed volume of equilibrated Glutathione Sepharose beads were added to the extract and incubated for 2 h. Beads were then washed four times with 25 CV Wash Buffer B2 (300 mM NaCl, 20 mM HEPES pH 7.6, 5 mM β-mercaptoethanol, 0.01% NP-40) before elution was achieved by protease cleavage. For this purpose, beads were resuspended in 1 CV Wash Buffer B3 (150 mM NaCl, 20 mM HEPES pH 7.6, 5 mM β-mercaptoethanol, 0.01% NP-40) and incubated together with 250 U GST-PreScission protease (MPIB Core Facility) for 18 h. The eluate was then adjusted to 300 mM NaCl and 6 mM imidazole for subsequent Ni-NTA affinity chromatography. Here, a bed volume of 1 mL equilibrated Ni-NTA Agarose (Qiagen) was added to the eluate and incubated for 1h. Beads were subsequently washed four times with 15 CV Wash Buffer B2 + 6 mM imidazole and five times with 2CV Wash Buffer B2 + 6 mM imidazole + 5% glycerol. Elution was then performed with Wash Buffer B2 + 250 mM imidazole. Fractions containing CDK were pooled and dialyzed by stirring two times against 300 volumes of Dialysis Buffer (150 mM NaCl, 50 mM HEPES pH 7.6, 0.1% NP-40, 2 mM β-mercaptoethanol, 10% glycerol) for 4 h in a Slide-A-Lyzer Dialysis Casette (Thermo Scientific). Dialysed material was recovered, aliquoted, snap-frozen and stored at -80°C.

Purification of bacterially expressed ^{GST}Sld2$^{1-150}$ variants

Bacteria carrying the expression plasmid were cultured in 1.5 L LB medium supplemented with antibiotics until mid-log phase. Chaperone expression was increased by incubation on ice for 10 min before protein expression was induced with 1 mM IPTG for 18 h at 20°C. Cells were harvested and resuspended in 35 mL Lysis Buffer B1 (500 mM NaCl, 50 mM HEPES pH 7.6, 5 mM β-mercaptoethanol, 0.01% NP-40, 100 µM AEBSF, 1x complete protease inhibitor cocktail EDTA-free (Roche)) and lysed with an EmulsiFlex-C3 system (Avestin) for three rounds at 1,000 bar. The lysate was then subjected to nucleic acid digestion by addition of 500 U Benzonase (Merck) and 2 mM $MgCl_2$ followed by incubation for 15 min at 4˚C. Cell debris was spun down at 140,000 g for 45 min. For glutathione affinity chromatography, 1 mL bed volume of equilibrated Glutathione Sepharose 4 FF (GE healthcare) was added to the extract and incubated for 2 h. Beads were then washed five times with 20 CV Wash Buffer B1 (250 mM NaCl, 20 mM HEPES pH 7.6, 5 mM β-mercaptoethanol, 0.01% NP-40) before elution was performed with Wash Buffer B1 + 20 mM glutathione. Elution fractions were pooled, brought to a conductivity of 10 mS/cm (100 mM salt) and subjected to anion exchange chromatography using a MonoQ 5/50 GL column (GE healthcare) with a salt gradient of 0.1 – 1 M NaCl over 20 CV. ^{GST}Sld2$^{1-150}$ containing fractions that eluted at conductivities of 28-32 mS/cm were pooled, aliquoted, snap-frozen and stored at -80°C.

Purification of bacterially expressed ^{GST}Dma1

Bacteria carrying the expression plasmid were cultured in 1 L LB medium supplemented with antibiotics until mid-log phase. Protein expression was induced with 1 mM IPTG overnight at 20°C. Cells were harvested and resuspended in 50 mL Lysis Buffer BP (500 mM NaCl, 50 mM HEPES pH 7.6, 10% glycerol, 0.1% NP-40, 2 mM β-mercaptoethanol, 1x complete protease inhibitor cocktail EDTA-free (Roche)) and lysed with an EmulsiFlex-C3 system (Avestin) for three rounds at 1,000 bar. PMSF was added to the lysate and cell debris was spun down at 46,500 g for 1 h. For glutathione affinity chromatography, 1 mL bed volume of equilibrated Glutathione Sepharose 4 FF (GE healthcare) was added to the extract and incubated for 2 h. Beads were then washed five times with 10 CV Lysis Buffer BP before elution was performed with Lysis Buffer BP supplemented with 20 mM glutathione. Elution fractions were pooled, brought to a conductivity of 10 mS/cm (100 mM salt) and subjected to anion exchange chromatography using a MonoQ 5/50 GL column (GE healthcare) with a salt gradient of 0.1 – 1 M NaCl over 20 CV. ^{GST}Dma1 containing fractions that eluted around 350mM NaCl, aliquoted, snap-frozen and stored at -80°C.

Purification of bacterially expressed ^{GST}Dma1^{FHA}

Bacteria carrying the expression plasmid were cultured in 1 L LB medium supplemented with antibiotics until mid-log phase. Chaperone expression was increased by incubation on ice for 10 min before protein expression was induced with 1 mM IPTG overnight at 20°C. Cells were harvested and resuspended in 50 mL Lysis Buffer BP (500 mM NaCl, 50 mM HEPES pH 7.6, 10% glycerol, 0.1% NP-40, 2 mM β-mercaptoethanol, 1x complete protease inhibitor cocktail EDTA-free (Roche)) and lysed with an EmulsiFlex-C3 system (Avestin) for three rounds at 1,000 bar. Cell debris was spun down at 10,000 g for 30 min. For glutathione affinity chromatography, 2 mL bed volume of equilibrated Glutathione Sepharose 4 FF (GE healthcare) were added to the extract and incubated for 2 h. Beads were then washed five times with 10 CV Lysis Buffer before elution was performed with Lysis Buffer + 20 mM glutathione. Elution fractions were pooled, brought to a conductivity of 10 mS/cm (100 mM NaCl) and subjected to anion exchange chromatography using a MonoQ 5/50 GL column (GE healthcare) with a salt gradient of 0.1 – 1 M NaCl over 20 CV. ^{GST}Dma1^{FHA} containing fractions were pooled, aliquoted, snap-frozen and stored at -80°C.

Purification of bacterially expressed ^{HIS}Dma1^{FHA}

Bacteria carrying the expression plasmid were cultured in 2 L LB medium supplemented with antibiotics until mid-log phase. Protein expression was induced with 1mM IPTG overnight at 18°C. Cells were harvested and resuspended in 100 ml Lysis Buffer LG (500 mM NaCl, 50 mM Tris-HCl pH 7.5, 10% glycerol, 0.1% NP-40, 2 mM β-mercaptoethanol, 1x complete protease inhibitor cocktail EDTA-free (Roche)). Subsequently cells were lysed with an EmulsiFlex-C3 system (Avestin) for three rounds at 1000 bar. After lysis, PMSF was added to the lysate and cells were centrifuged for 1 h at 40,000 rpm (4°C) to spin-down cell debris. Supernatant was then supplemented with 20 mM imidazole, incubated with 2 ml bed volume NiNTA agarose (Qiagen) previously washed with Lysis Buffer LG, and let stirring for 2h at 4°C. NiNTA agarose was then washed three times with 10 CV Lysis Buffer LG + 20 mM Imidazole before elution was performed with Lysis Buffer LG + 250 mM imidazole. Eluted fractions were pooled together and subjected to size exclusion chromatography using HiLoad 16/600 Superdex 200 pg (GE healthcare). Eluted fractions were then pooled, brought to a salt concentration of 50 mM NaCl and subjected to cation exchange chromatography using MonoS 5/50 GL Column (GE healthcare) with a salt gradient of 0.05-1 M NaCl over 20 CV. Fractions containing Dma1 N-FHA were pooled and salt concentration was brought to 170 mM NaCl, before the protein was aliquoted, snap-frozen and stored at -80°C.

Purification of Mck1 and Cdc5 from *S. cerevisiae*

YFZ019 and YFZ020 were grown in 10 L YP medium + 2% raffinose at 30°C until mid-log phase before expression was induced by addition of 2% galactose. After 4 h of induction, yeast cells were harvested and washed twice with 250 mL 1 M Sorbitol + 25 mM HEPES pH 7.6. The pellet was resuspended in 1 volume of Lysis Buffer Y1 (500 mM NaCl, 100 mM HEPES pH 7.6, 0.1% NP-40, 10% glycerol, 2 mM β-mercaptoethanol, 400 µM PMSF, 4 µM aprotinin, 4 mM benzamidin, 400 µM leupeptin, 300 µM pepstatin A, 4x complete protease inhibitor cocktail, EDTA-free) and frozen drop-wise in liquid nitrogen. Frozen cell drops were crushed using a freezer/mill system (Spex Sample Prep). Cell powder was thawed on ice and centrifuged at >185,000 g for 1 h. The clear phase was recovered and incubated with 1 ml bed volume of anti-FLAG M2 resin (Sigma) equilibrated in Lysis Buffer Y1. After 2h of incubation, the resin was washed five times with 10 CV of Wash Buffer Y1 (500 mM NaCl, 100 mM HEPES pH 7.6, 0.1% NP-40, 10% glycerol, 2 mM β-mercaptoethanol). Two elution steps were performed by adding 1 CV 0.5 mg/mL 3FLAG peptide in Wash Buffer Y1 and incubation for 30 min. Obtained fractions were pooled, brought to a conductivity of 10 mS/cm (100 mM salt) and subjected to anion exchange chromatography using a MonoQ 5/50 GL column with a salt gradient of 0.1 – 1 M NaCl over 20 CV. $Cdc5^{3FLAG}$ eluted at a conductivity of ~15 mS/cm and $Mck1^{3FLAG}$ at ~20 mS/cm. Kinase containing fractions were aliquoted, snap-frozen and stored at -80°C.

Purification of DDK from *S. cerevisiae*

DDK was purified as described previously (Gros et al., 2014) with modifications. YFZ021 cells were grown in 10 L YP medium + 2% raffinose at 30°C until mid-log phase before expression was induced by addition of 2% galactose. After 4 h of incubation, yeast cells were harvested and washed twice with 250 mL 1 M Sorbitol + 25 mM HEPES pH 7.6. The pellet was resuspended in 1 volume of Lysis Buffer Y2 (400 mM NaCl, 100 mM HEPES pH 7.6, 0.1% NP-40, 10% glycerol, 2 mM β-mercaptoethanol, 400 µM PMSF, 4 µM aprotinin, 4 mM benzamidin, 400 µM leupeptin, 300 µM pepstatin A, 4x complete protease inhibitor cocktail EDTA-free) and frozen drop-wise in liquid nitrogen. Frozen cell drops were crushed using a freezer/mill system. Cell powder was thawed on ice and centrifuged at >185,000 g for 1 h. The clear phase was recovered and incubated with 1 ml bed volume of anti-FLAG M2 resin (equilibrated in Lysis Buffer Y2). After incubation for 2 h at 4°C, the resin was washed six times with 2 CV Wash Buffer Y2 (400 mM NaCl, 100 mM HEPES pH 7.6, 0.1% NP-40, 10% glycerol, 2 mM β-mercaptoethanol). For λ-phosphatase treatment, beads were resuspended in 1 CV Wash Buffer Y2 + 2mM $MnCl_2$ + 900 U λ-phosphatase (New England Biolabs) and incubated for 1h at 30°C in a tabletop thermoshaker. Beads were recovered and bound DDK was eluted twice with 1 CV 0.5 mg/ml 3FLAG peptide in Wash Buffer Y2 for 30 min. Elutions were pooled, concentrated using a Vivaspin 500 MWCO 50.000 (GE healthcare) and fractionated by size exclusion chromatography using a Superdex 200 GL 10/300 column (GE healthare, equilibrated in Wash Buffer Y2) over 1.2 CV. DDK containing fractions were pooled, brought to a conductivity of 10 mS/cm (100 mM salt) and fractionated by anion exchange chromatography using a MonoQ 5/50 GL column with a salt gradient of 0.1 – 1 M NaCl over 20 CV. DDK containing fractions eluted at ~24-26 mS/cm and were aliquoted, snap frozen and stored at -80°C.

In vitro kinase assays

Kinase assays using purified $^{GST}Sld2^{1-150}$ variants

Kinase assays were performed as described previously (Mordes et al., 2008; Pfander et al., 2011) with minor modifications. Briefly, 20 pmol GST or $^{GST}Sld2^{1-150}$ variants bound to GSH affinity beads (GE healthcare, ThermoFisher Scientific) were used as substrates in Kinase Buffer (100 mM KOAc, 10 mM HEPES pH 7.6, 50 mM β-glycerophosphate, 10 mM $MgCl_2$, 5mM $Mg(OAc)_2$, 2 mM β-mercaptoethanol) in a 50 µL reaction volume containing 10 pmol of kinase and 5 µg BSA. Reactions were started by addition of 1 mM ATP + 5 µCi γ[^{32}P]-ATP (PerkinElmer) and incubated 30 min at 30°C in a tabletop shaker. Reactions were stopped by adding Laemmli sample buffer followed by boiling at 95°C. Proteins were separated by SDS-PAGE and analyzed by Coomassie Brilliant Blue staining and autoradiography using a Typhoon FLA 9500 imager (GE healthcare).

For sequential phosphorylation reactions of $^{GST}Sld2^{1-150}$ variants, bead-bound substrates were treated as described above without addition of γ[^{32}P]-ATP. After 30 min at 30°C, beads were recovered, successively washed with 500 µL Binding Buffer A (200 mM KOAc, 100 mM HEPES pH 7.6, 0.02% NP-40, 2 mM β-mercaptoethanol, 10% glycerol) and 500 µL Binding Buffer B (100 mM KOAc, 100 mM HEPES pH 7.6, 0.02% NP-40, 2 mM β-mercaptoethanol, 10% glycerol) to remove unbound reaction components. Consecutive kinase reactions with γ[^{32}P]-ATP were performed as described above.

Kinase assays using synthetic Sld2$^{118-143}$ peptides

To control for peptide input levels, 75 µL suspension of Dynabeads M-280 Streptavidin (Sigma) were equilibrated with Binding Buffer C (500 mM KOAc, 100 mM HEPES pH 7.6, 0.02% NP-40, 2 mM β-mercaptoethanol, 10% glycerol) and incubated with a saturating amount (12.5 µg) of desthiobiotinylated Sld2$^{118-143}$ peptide. After peptide binding, beads were washed twice with 500 µL Binding Buffer C and once with 500 µL Binding Buffer B before kinase reactions were performed as described above.

Mass spectrometric analysis of in vitro kinase reactions

For phosphorylation site mapping of in vitro reactions, assays were performed with Kinase Buffer in a 500 µL reaction volume containing 200 pmol of ^{GST}Sld2$^{1-150}$, 100 pmol of respective kinase and 50 µg BSA. Reactions were started by addition of 1 mM ATP and incubated 30 min at 30°C and stopped by TCA precipitation. Samples from precipitated proteins were generated using HU buffer. Samples were split equally, separated by SDS-PAGE and subjected to in-gel digestion by both LysC and GluC. Gel slices were dissolved and analyzed by LC-MS/MS using a LTQ Orbitrap mass spectrometer. Data was analysed with MaxQuant (Cox and Mann, 2008).

Fluorescence anisotropy measurements

Peptides were labelled with 5- (and 6-) carboxyfluorescein (mixed isomers) at the N-terminus and incubated at a final concentration of 10nM with increasing concentrations of ^{HIS}Dma1^{FHA} in 50 µl reactions for 1h at 4°C before measuring using a Genios Pro (Tecan). The reaction buffer contained: 170 mM NaCl, 50 mM Tris-HCl pH 7.5, 10% glycerol, 0.02% NP-40 and 2 mM β-mercaptoethanol. The excitation and emission wavelengths were respectively 485nm and 535 nm. Each titration point was measured three times using ten reads with an integration time of 40µs. Polarization data were analyzed using BIOEQS software (Royer, 1993) by non-linear regression fitting with a one-site total binding model. Background fluorescence from wells containing only buffer and peptide was subtracted from all the values.

Microscale thermophoresis measurements

Peptides were labelled with 5- (and 6-) carboxyfluorescein (mixed isomers) at the N-terminus and incubated at a final concentration of 20 nM with increasing concentrations of ^{HIS}Dma1^{FHA} in 20 µl reactions. Samples were incubated for 1h at 4°C before measuring with a blue/red Monolith NT.115 (NanoTemper Technologies) using the blue filter set. Each measurement was performed at 20% MST power and 40% LED power, with pre-MST period of 5 s, MST acquisition period of 30 s and post-MST period of 5 s, by using standard treated capillaries at room temperature. The reaction buffer contained: 170 mM NaCl, 50 mM Tris-HCl pH 7.5, 10% glycerol, 0.02% Tween-20, 1% BSA and 2 mM β-mercaptoethanol. Data were analysed by using the Affinity Analysis (MST) V2.0.2 software (NanoTemper Technologies). The unbound fraction value given from the instrument was subtracted from each data-set. Data were plotted using non-linear fitting with a one-site total binding model.

Peptide pulldowns

To control for peptide input levels, 75 µL suspension of Dynabeads M-280 Streptavidin (Sigma) were equilibrated with Binding Buffer C (500 mM KOAc, 100 mM HEPES pH 7.6, 0.02% NP-40, 2 mM β-mercaptoethanol, 10% glycerol) and incubated with a saturating amount (12.5 µg) of desthiobiotinylated Sld2$^{118-143}$ peptide. After peptide binding, beads were washed twice with 500 µL Binding Buffer C before addition of an equal volume of Binding Buffer C containing 1 µg ^{GST}Dma1 or ^{GST}Dma1^{FHA} together with 1 µg GST. After 1 h incubation, the beads were washed four times and then eluted by boiling in Laemmli buffer. Peptide pulldowns with ^{HIS}Dma1^{FHA} (1 µg recombinant protein incubated with 12.5 µg peptide) were performed with Binding Buffer A (100 mM HEPES pH 7.6 (KOH), 200 mM KOAc; 10% glycerol, 0.02% NP-40, 2 mM β-mercaptoethanol) instead of Binding Buffer C.

Acrylamide gel electrophoresis and western blot analysis

Protein samples were separated by standard SDS-polyacrylamide gel electrophoresis. If not stated otherwise, 4-12% Novex NuPAGE Bis-Tris precast gels (ThermoFisher) were used with MOPS buffer (50 mM MOPS, 50 mM Tris-base, 1.025 mM EDTA, 0.1% SDS, adjusted to pH 7.7). SDS-PAGE running buffer (25 mM Tris, 192 mM glycine, 0.1% SDS) was used for electrophoresis of handcast gels supplemented with phos-tag reagent AAL-107 (Wako Chemicals). The conditions to separate phosphorylation-dependent shifts of replication factors are given below.

After electrophoresis, proteins were transferred to a nitrocellulose membrane (Amersham Protran Premium 0.45 µM NC) using a tank blotting system. Membranes were incubated with primary antibodies at 4°C overnight. Incubation with appropriate secondary antibodies coupled to horseradish peroxidase (HRP) was performed at room temperature for 3 h. Membranes were washed five times for 5 min with western wash buffer (50 mM Tris pH 7.5, 137 mM NaCl, 3 mM KCl, 0.2 % NP-40) and incubated with Pierce ECL western blotting substrate (ThermoFisher) according to the instructions of the manufacturer. Chemiluminescence was detected with a LAS-3000 image reader (FujiFilm).

Conditions to detect phosphorylation-dependent shifts

Protein	Used gel / buffer
Mcm3-3FLAG	6% acrylamide gel + 15 µM phos-tag AAL-107 SDS-PAGE running buffer
Orc6	10% acrylamide gel / SDS-PAGE running buffer
Rad53	10% acrylamide gel / SDS-PAGE running buffer
Sld2	12% Novex NuPAGE Bis-Tris gel / MOPS buffer
Sld3-9myc	6% acrylamide gel + 10 µM phos-tag AAL-107 SDS-PAGE running buffer

Antibodies used in this study:

Antibody	Target protein	Host organism	Source
JD147	Rad53	Rabbit	John Diffley
sc-6733	Cdc5	Goat	Santa Cruz
sc-9071	Clb2	Rabbit	Santa Cruz
ANTI-FLAG M2	FLAG-tag	Mouse	Sigma-Aldrich
Anti-Sld2	Sld2	Rabbit	Philip Zegerman
SB49	Orc6	Mouse	Bruce Stillman / John Diffley
4A6	myc-tag	Mouse	Millipore
9H8/5	Cdc6	Mouse	abcam
22C5D8	Pgk1	Mouse	Invitrogen
sc-459	GST	Rabbit	Santa Cruz
sc-8017 (P4D1)	Ubiquitin	Mouse	Santa Cruz
sc-1663	Gal4-AD	Mouse	Santa Cruz
sc-5705	Dbf4	Goat	Santa Cruz
06-719	lexA-BD	Rabbit	EMD Millipore

Quantification of western blots and curve fitting

Western blots were analysed using the ImageJ-based software package Fiji (http://fiji.sc/FIJI (Schindelin et al., 2012)). For CHX chases, the levels of Sld2 were quantified and, in case of unequal loading, normalized to the levels of Pgk1. To avoid the introduction of an additional source of errors, normalization was omitted if the loading of the gels was homogeneous as judged by unspecific bands or Ponceau staining.

Subsequently, the data was analysed and fitted using the software Origin Pro 8.0 (OriginLab Corp.). Data from CHX shut-off experiments was approximated with an exponential function (Equation (1)) for better visualization. Data from release experiments were approximated with a logistic function (Equation (2)). Coefficients of determination (R^2) for the logistic functions were between 0.94 and 0.99 except for the Orc6 curve in Fig. 1C ($R^2 = 0.87$) and the Orc6 curve in Fig. S6B ($R^2 = 0.88$).

Equation (1) – Exponential function

$$f(t) = \exp(-A\,t)$$

Equation (2) – Logistic function

$$f(t) = \frac{1}{1 + \exp\left(-k\left(t - t_{\frac{1}{2}}\right)\right)}$$

Mass spectrometric analysis of in vivo Sld2 phosphorylation sites

Sld2 phosphorylation sites were determined by mass spectrometry-based label free quantification of phosphopeptides from $Sld2^{3FLAG}$ enriched by pulldown from yeast lysate. To this end, endogenous $Sld2^{3FLAG}$ or $Sld2^{3FLAG}$ expressed from the strong GPD promoter was used; the latter yielded more reproducible detection of low abundant Sld2 peptides with higher order phosphorylation.

For each sample, 2 L cultures were used, grown to a density of $1x10^7$ cells/ml and arrested in G1 with α-factor or in mitosis with nocodazole. For the experiment in Fig. S3F, four independent biological replicates were used. Lysates were prepared using a freezer mill in buffer MS (200 mM KOAc, 100 mM HEPES pH 7.6, 0.1% NP-40, 10% glycerol, 2 mM β-mercaptoethanol, 10mM NaF, 20mM β-glycerophosphate, 400 µM PMSF, 4 µM aprotinin, 4 mM benzamidin, 400 µM leupeptin, 300 µM pepstatin A, 4x complete protease inhibitor cocktail, EDTA-free). FLAG-pulldown was performed using FLAG-M2-agarose (Sigma) and elution with 3xFLAG peptide. Eluates were concentrated by TCA precipitation and separated on a 4-12% NuPAGE Bis-Tris gel (Invitrogen). The gel was stained with GelCode Blue (Thermo Scientific) and one gel slice containing the Sld2 band was excised and analysed by LC-MS/MS after in-gel Lys-C digestion. Samples were measured on a Q-Exactive Hybrid Quadrupole-Orbitrap MS and analysed using MaxQuant (Cox and Mann, 2008).

SUPPLEMENTAL REFERENCES

Bishop, A.C., Ubersax, J.A., Petsch, D.T., Matheos, D.P., Gray, N.S., Blethrow, J., Shimizu, E., Tsien, J.Z., Schultz, P.G., Rose, M.D., et al. (2000). A chemical switch for inhibitor-sensitive alleles of any protein kinase. Nature *407*, 395–401.

Cox, J., and Mann, M. (2008). MaxQuant enables high peptide identification rates, individualized ppb-range mass accuracies and proteome-wide protein quantification. Nature biotechnology *26*, 1367-1372.

Janke, C., Magiera, M.M., Rathfelder, N., Taxis, C., Reber, S., Maekawa, H., Moreno-Borchart, A., Doenges, G., Schwob, E., Schiebel, E., et al. (2004). A versatile toolbox for PCR-based tagging of yeast genes: new fluorescent proteins, more markers and promoter substitution cassettes. Yeast *21*, 947–962.

Mordes, D. A., Nam, E. A., and Cortez, D. (2008). Dpb11 activates the Mec1–Ddc2 complex. Proceedings of the National Academy of Sciences *105*, 18730-18734.

Putnam, C.D., and Kolodner, R.D. (2010). Determination of gross chromosomal rearrangement rates. Cold Spring Harbor Protocols *2010*, pdb.prot5492.

Rosche, W.A., and Foster, P.L. (2000). Determining mutation rates in bacterial populations. Methods *20*, 4–17.

Rothstein, R. J. (1983). One-step gene disruption in yeast. *Methods in enzymology 101*, 202-211.

Royer, C.A. (1993). Improvements in the numerical analysis of thermodynamic data from biomolecular complexes. Anal. Biochem. *210*, 91–97.

Schindelin, J., Arganda-Carreras, I., Frise, E., Kaynig, V., Longair, M., Pietzsch, T., Preibisch, S., Rueden, C., Saalfeld, S., Schmid, B., et al. (2012). Fiji: an open-source platform for biological-image analysis. Nature methods *9*, 676-682.

Stewart, F.M. (1994). Fluctuation tests: how reliable are the estimates of mutation rates? Genetics *137*, 1139–1146.